GA–A22068
CONF-9506282--3

RADIATION DISTRIBUTIONS IN DETACHED DIVERTOR OPERATION ON DIII–D

by

A.W. LEONARD, S.L. ALLEN, M.E. FENSTERMACHER, D.N. HILL, C.J. LASNIER, W.M. MEYER, T.W. PETRIE, J.G. WATKINS, R.D. WOOD, AND THE DIII–D TEAM

JULY 1995

GENERAL ATOMICS

GA–A22068

RADIATION DISTRIBUTIONS IN DETACHED DIVERTOR OPERATION ON DIII–D

by

A.W. LEONARD, S.L. ALLEN,* M.E. FENSTERMACHER,* D.N. HILL,* C.J. LASNIER,* W.M. MEYER,* T.W. PETRIE, J.G. WATKINS,† R.D. WOOD,* AND THE DIII–D TEAM

This is a preprint of a paper presented at the 22nd European Conference on Controlled Fusion and Plasma Physics, June 3–7, 1995, in Bournemouth, United Kingdom, and to be published in the *PROCEEDINGS.*

*Lawrence Livermore National Laboratory.
†Sandia National Laboratory.

Work supported by
U.S. Department of Energy
under Contract Nos. DE-AC03-89ER51114, W-7405-ENG-48,
and DE-AC04-94AL85000

GA PROJECT 3466
JULY 1995

GENERAL ATOMICS

RADIATION DISTRIBUTIONS IN DETACHED DIVERTOR OPERATION ON DIII–D*

A.W. Leonard, S.L. Allen,† M.E. Fenstermacher,† D.N. Hill, † C.J. Lasnier, †
W.M. Meyer,† T.W. Petrie, J.G. Watkins,Δ R.D. Wood,† and The DIII–D Team

General Atomics, P.O. Box 85608, San Diego, CA 92138-9784

Enhanced radiative losses with accompanying divertor heat flux reductions have been achieved on DIII–D by the puffing of deuterium and/or neon gas [1]. In addition these highly radiating, reduced divertor heat flux regimes have been extended to lower core plasma density through cryopumping in the divertor. This paper describes the magnitude, distribution and other characteristics of the radiation obtained during these experiments. Radiated power is measured by two poloidally separated 24-channel bolometer arrays. One array views from above, the other from below the midplane. The radiated power profile is reconstructed by assuming constant emissivity on a flux surface for the core and SOL plasma and parameterizing the divertor radiation by flux surface and distance above the divertor floor [2]. Images of visible line radiation in the divertor provide information about the distribution of impurities; *e.g.*, a tangential image is inverted to provide a poloidal profile of the emissivity. The core plasma impurity densities are measured by charge-exchange spectroscopy techniques.

1. Deuterium Injection

The target plasma for the gas injection experiments is a 1.6 MA, 2.1 T single-null ELMing H–mode plasma with ~8 MW of injected power and the ∇B drift direction toward the X-point. With no additional gas puffing IR cameras measure the highest heat flux at the outboard strikepoint at ~6.0 MW/m^2 but ≤1.0 MW/m^2 at the inboard strikepoint. Conversely, the divertor radiation is much greater in the inboard divertor than the outboard [3]. This radiation pattern obtained from inversion of the bolometer data, is shown in Fig. 1(a). Sufficient deuterium puffing, ~100 torr-ℓ/s for ~500 ms, produces an abrupt transition to a highly radiating state in the outboard divertor [4]. The increased radiation in the outboard divertor [Fig. 1(b)] extends from the X-point to the divertor target peaking at ~10 W/cm^3. This radiating state is also characterized by a drop in peak outboard divertor heat flux by a factor of 3–5 and a decrease in plasma flux and pressure at the strikepoint as measured by Langmuir probes. In the inboard divertor there is no significant change after the transition. Through the transition the plasma remains in H–mode with confinement at ~2 x L–mode.

By summing specific regions of the reconstructed radiation profile, loss channels for the injected power can be identified. Before puffing, 18%–20% of the injected power is lost

*Work supported by the U.S. Department of Energy under Contract Nos. DE-AC03-89ER51114, W-7405-ENG-48, and DE-AC04-94AL85000.

†Larwrence Livermore National Laboratory.

ΔSandia National Laboratory.

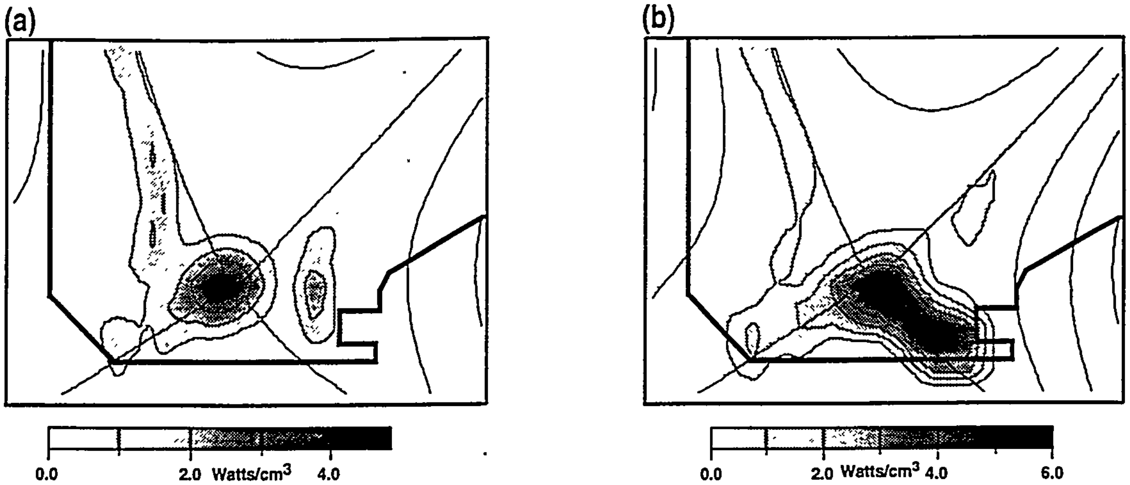

Fig.1. Divertor radiation distribution for (a) no additional gas puffing and (b) deuterium puffing until radiative regime obtained

through radiation in the core and SOL. In the divertor, radiation accounts for another ~30% of the power with most of that in the inboard side. The balance of the injected power is observed as divertor plate heat flux, with ≥3/4 of that in the outboard strike-point. A detailed accounting of power balance during ELMing H–mode in DIII–D is given in Ref. [3]. After injection, the outboard divertor radiation increases from 7% of the injected power to 30%. With the extra gas there is a moderate increase in central density, from 7.8×10^{19} m^{-3} to 8.9×10^{19} m^{-3} while the core and SOL radiation modestly increase from 19% to 23% of the injected power. The increase in total radiation is offset by a corresponding decrease in divertor heat flux. A summary of radiation distribution is presented below.

	No Gas	D_2 Puffing	D_2 with Pumping
Core & SOL	20%	23%	23%
Outboard Divertor	7%	31%	31%
Inboard Divertor	21%	16%	21%
Total Radiation	48%	71%	76%

The fractional contributions to radiation from neutral hydrogen and impurities have not yet been measured on DIII–D. With complete graphite coverage carbon is expected to be the dominant impurity. Carbon concentrations of ~1.5% have been measured in the core plasma by charge-exchange spectroscopy for these discharges. Inverted poloidal profiles of visible CIII emission from camera images present a pattern similar to that for radiated power. Visible CIII emission is concentrated along the inner leg of the divertor before deuterium puffing, but then increases to a greater level along the outboard divertor after the radiative transition. Given the measured carbon concentrations and the region of highly radiating CIII, the intrinsic carbon impurity probably represents a significant fraction of the increase in radiated power. Measurements on JT-60U have shown that carbon contributes approximately half of the radiation observed during highly radiating divertor discharges [5]. Measurements of these contributions on DIII–D are planned for the future.

Divertor pumping on DIII–D has allowed operation of ELMing H–mode plasmas at lower central density [6]. Puffing of deuterium into these pumped plasmas has produced a similar increase in divertor radiation and reduction in heat flux as the non-pumped case. These plasmas have a ~25% lower core density and maintain good H–mode confinement. The divertor radiation profile, shown in Fig. 2, while yielding the same total power has a more even distribution of radiation along the inboard and outboard divertor legs. Otherwise the magnitude and distribution of radiation are very similar. This result represents a significant step in the effort to independently control the core and divertor plasmas.

2. Neon Injection

Puffing of neon gas has also been effective in reducing peak divertor heat flux. For neon puffing the increase in radiation occurs inside the separatrix. With sufficient neon to produce a heat flux reduction of a factor of 3–5, the radial profile of the radiative emissivity peaks at 0.5 W/cm^3 just inside the separatrix, from ρ = 0.8–1.0, as shown, in Fig. 3. A core neon concentration of 1.5% for this case was measured in the central plasma. The total radiation increases to 65%–70% of the injected power. The mantle of radiation inside the separatrix is roughly equal in magnitude to the divertor/X-point radiation. A radiation distribution summary is given in Table I. The total divertor radiation decreases somewhat and moves up the divertor

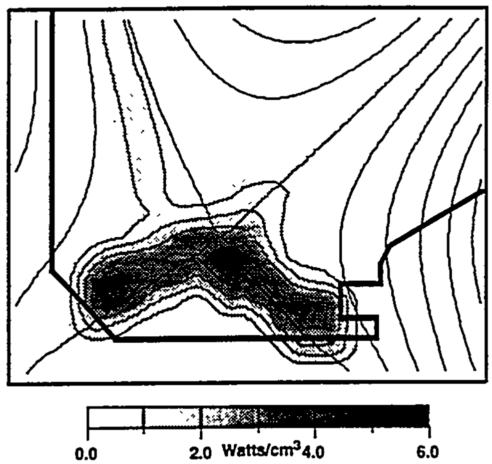

Fig. 2. Divertor radiation in radiative regime at lower density with pumping.

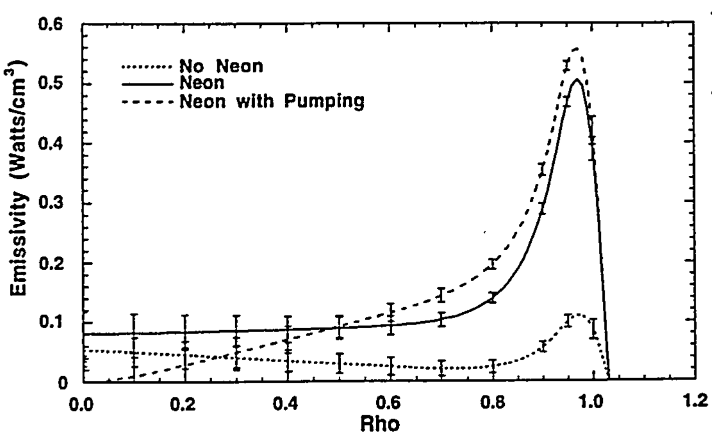

Fig. 3. Radial profile of radiative emissivity in core plasma with no gas puffing, neon injection and neon injection with pumping.

Table 1

Radiative Power Loss	Neon Injection	Neon with Pumping
Core &SOL	42%	48%
Mantle, ρ = 0.8–1.0	24%	33%
X-point/ divertor	23%	21%
Total Radiation	65%	69%

leg into the X-point region. The divertor radiation distribution is illustrated in Fig. 4. Visible CIII images show a decrease in emissivity in the X-point region. Though significant power is lost inside the separatrix, H–mode confinement is maintained. However, the ELM character is strongly affected, with the ELMs decreasing in frequency to ~5–10 Hz and increasing in amplitude to produce a strong modulation in the central plasma density of ~15%.

Divertor pumping has also been applied to neon injection. When injecting neon into a pumped plasma with 25% lower central density, a similar mantleof radiation and heat flux reduction is produced as for the nonpumped case. The core radiation profile is also shown in Fig. 3. The X-point/divertor radiation, though remaining similar in magnitude to the nonpumped plasma, moves back to the inboard leg of the divertor. The ELMs are again reduced in frequency and of larger amplitude producing a significant modulation of the main plasma density. A method of ELM control must be found, such as in the ASDEX-U CD H–mode [7], in order to practically make use of edge plasma radiation for power dissipation.

3. Conclusion

Attractive methods of reducing peak divertor peak divertor heat flux have been demonstrated by the injection of either deuterium or neon gas. With deuterium injection the radiation is extended along the divertor leg effectively dissipating much of the injected power. Much of the increased radiation likely comes from the intrinsic carbon impurity. More modeling is needed to determine if such a scenario can be utilized in larger size devices. The attainment of a highly radiating divertor at reduced central plasma density is also encouraging. This implies a flexibility to optimize the core plasma conditions yet maintain a reduced divertor heat flux if the right conditions are met.

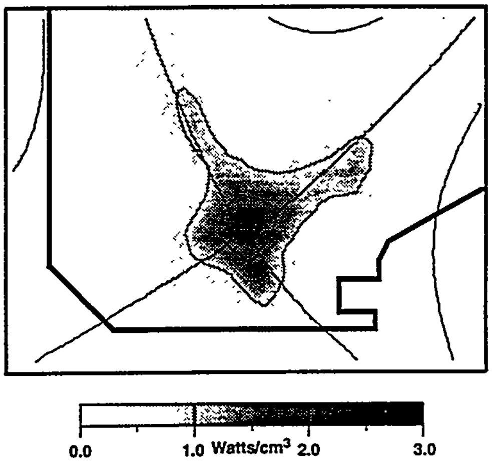

Fig. 4 Divertor radiation distribution with neon injection

Neon injection has demonstrated the possibility of radiating power inside the separatrix before it reaches the divertor. Better understanding and control of the relationship between H–mode power threshold, ELM characteristics and plasma density are needed to asses the applicability of this scenario for ITER-sized tokamaks.

[1] Petrie T W, Buchenauer D, Hill D N et al., *J Nucl. Mater.* **196-198** 848 (1992)

[2] Leonard A W et al., *Rev. Sci Instrum.* **66** 1201 (1995)

[3] Leonard A W,et al., Proc 11th Conf. Plasma Surface Interaction, Mito (Japan) 1994

[4] Petrie T W et al., submitted to Nucl. Fusion

[5] Kubo H., et al., *Nucl. Fusion* **10** 1427 (1993)

[6] Mahdavi M A et al., Proc of 20th EPS Conference on Controlled Fusion and Plasma Physics, Lisbon (Portugal) Vol. **17C**, Part II 647 (1993)

[7] Gruber O, Kallenbach A, Kaufmann M submitted to Phys. Rev. Lett.